Optimized Fractional Order Integral-Tilt Derivative Controller for Frequency Regulation of Interconnected Diverse Renewable Energy Resources

AMIL DARAZ[1], SUHEEL ABDULLAH MALIK[1], AHMAD TAHER AZAR[2,3,4], (Senior Member, IEEE), SHERAZ ASLAM[3,5], (Member, IEEE), TAMIM ALKHALIFAH[6], AND FAHAD ALTURISE[6]

[1]Department of Electrical Engineering, FET, International Islamic University, Islamabad, Islamabad 44000, Pakistan
[2]College of Computer and Information Sciences, Prince Sultan University, Riyadh 12435, Saudi Arabia
[3]Automated Systems and Soft Computing Laboratory (ASSCL), Prince Sultan University, Riyadh 12435, Saudi Arabia
[4]Faculty of Computers and Artificial Intelligence, Benha University, Benha 13511, Egypt
[5]Department of Electrical Engineering, Computer Engineering, and Informatics, Cyprus University of Technology, 3036 Limassol, Cyprus
[6]Department of Computer, College of Science and Arts in Ar Rass, Qassim University, Ar Rass, Qassim 52571, Saudi Arabia

Corresponding authors: Amil Daraz (amil.phdee108@iiu.edu.pk); Sheraz Aslam (sheraz.aslam@cut.ac.cy); and Ahmad Taher Azar (ahmad.azar@fci.bu.edu.eg, aazar@psu.edu.sa)

ABSTRACT The interconnection of renewable energy systems, which are complex nonlinear systems, often results in power fluctuations in the interconnection line and high system frequency due to insufficient damping in extreme and dynamic loading situations. To solve this problem, load frequency control ensures nominal operating frequency and orderly fluctuation of grid interconnection power by delivering high-quality electric power to energy consumers through efficient and intelligent control systems. To introduce the frequency control of power systems, this paper presents a novel control technique of Fractional Order Integral-Tilt Derivative with Filter (FOI-TDN) controller optimized by the current soft computing technique of hybrid Sine-Cosine algorithm with Fitness Dependent Optimizer (hSC-FDO). For more realistic analysis, practical constraints with nonlinear features, such as controller dead band, communication time delay, boiler dynamics, and generation rate constraint are embedded in the given system model. The proposed approach outperforms some recently developed heuristic approaches such as fitness dependent optimizer, firefly algorithm, and particle swarm optimization for the interconnected power system of two areas with multiple generating units in terms of minimum undershoot, overshoot, and settling time. To improve the system performance, capacitive energy storage devices are used in each area and thyristor control phase shifter is used in the interconnection line of the power system. The potential of the hSC-FDO-based FOI-TDN is demonstrated by comparing it with conventional FOTID/FOPID/PID controllers for two areas with multiple power generators IPS. Finally, a robustness analysis is performed to determine the robustness of the presented control system by varying the system loads and system parameters.

INDEX TERMS Automatic generation control, fractional order controller, hybrid sine cosine, fitness dependent optimizer, load frequency control, renewable energy resources.

I. INTRODUCTION

Maintaining the stability and security of interconnected modern power systems (PSs) has become an effective tool for additional services. These amenities provide uninterrupted power supply and ensure the quality of electricity. Frequency

The associate editor coordinating the review of this manuscript and approving it for publication was Salvatore Favuzza.

stabilization is an important indicator of power quality. Load-frequency control (LFC) plays a crucial role in the operation and control of the PS and ensures the generation of high-quality electricity [1], [2]. With the help of LFC, the operating point of the power generation system is adjusted to match the amount of power generated under different load scenarios. In this way, an attempt is made to reduce frequency fluctuations in the system area. An intelligent and advanced

Acronym	Definition
AGC	Automatic Generation Control
LFC	Load Frequency Control
TID	Tilted Integral Derivative
PID	Proportional Integral Derivative
FOPID	Fractional Order Proportional Integral Derivative
FOI-TD	Fractional Order Integral Tilted- Derivative
CTD	Communication Time Delay
BD	Boiler Dynamics
GRC	Generation Rate Constraint
TD	Time Delay
GDB	Governor Deed Band
IPS	Interconnected Power System
FLC	Fuzzy Logic Controller
FOC	Fractional Order Controller
FDO	Fitness Dependent Optimizer
I-FDO	Improved-Fitness Dependent Optimizer
TLBO	Teaching Learning Based Optimization
PSO	Particle Swarm Optimization
TF	Transfer Function
Osh	Overshoot Time
Ush	Undershoot Time
SLP	Step Load Perturbation
Kr	Steam Turbine Constant
T12	Synchronization Coefficient
ITSE	Integral Time Square Error
Tt	Turbine Time Constant
IAE	Integral Absolute Error
ISE	Integral Square Error
ITAE	Integral Time Absolute Error
GDZ	Governor Dead Zone
λ	Fractional Integrator Order
n	Tilt non zero real number
N	Filter
μ	Fractional derivative order
δF	System frequency deviation
$\delta ptie$	Tie-line power deviation
T_W	wind turbine constant
T_g	Governor time constant
R	Droop constant
T_{p1}	Power system constant
Kt	Tilted gain
β	Pitch angle
K_{p1}	Power system gains

LFC control structure is required to balance the effects of load fluctuations and maintain a certain range of generation, system frequency, and power flow in the interconnected grid. [3]–[5].

A. LITERATURE REVIEW

To improve dynamic efficiency, the LFC employs a variety of control mechanisms. Simple conventional controllers are the most commonly used LFC controllers in the industry because they are simple in structure, easy to implement, inexpensive, and well designed [6], [7]. The PID controller and its various modified forms are mostly used in AGC analysis [8]. Daraz [9] employed an I-PD for the AGC of two areas IPS with multi-generation units and showed that it outperforms the PID and PI controllers. The authors in [10] compared the performance of PID with a double derivative controller for an LFC system with the performance of I/ PI /PID controllers. The superior transient response under truly constrained conditions such as GRC, GDZ, CTD, and BD is not guaranteed by standard controllers. Due to the wide range of load

magnitudes, the basic approaches of standard controllers are ineffective for acceptable dynamic output. The use of artificial neural networks and fuzzy logic controllers for the AGC system was also investigated in [11]. Compared to traditional controllers, the FLC-based LFC system optimizes the system outputs by selecting the rule base, membership features, scaling factor, and defuzzification mechanism. In contrast, FLC and ANN database analysis and training require a significant amount of processing time.

On the other hand, fractional order (FO) controllers are becoming more popular due to their adaptability and greater degree of freedom. In most cases, this leads to additional tuning requirements as new pole types are added, such as hyper-damped poles. This means that the stability range has been extended, allowing us to develop more flexible controllers. As a result, researchers have shown a strong interest in FO controllers (FOCs). In [12], [13], FOCs have been applied to a variety of electrical systems. A tilt-integral-derivative (TID) controller is also a member of the FOC family and has been used recently to solve LFC problems. The advantages of the TID controller include its ability to adjust the parameters of a closed-loop system, its robustness, and its greater ability to reject disturbances. As a result, several research papers have recommended the TID controller as a means of solving LFC problems [14], [15]. To take advantage of TID and FOPID controllers, Morsali *et al.* [16] proposes a hybrid controller based on their combination. Moreover, the configuration of the cascade controller (CC) was preferred to the configuration of the non cascade controller due to its advantages. Better results can be obtained if the cascaded controller has more adjustment knobs than a non-crude cascaded controller. Thus, the CC structure is one of the most successful controller strategies to improve the defence performance of a control system in control applications, especially when disturbances occur [17]. As a result, several variants of the cascaded controller have been used to improve the frequency stability of power systems [18], [19]. However, no performance evaluation of FOI-TDN structured controller has been discovered so far. Considering these facts, a proposed control strategy for multi-area AGC IPS models are presented.

To achieve optimal LFC of the power system, the design of the controller alone is not sufficient. Optimization strategies to determine the parameters of the controller are equally important in the field of LFC. Researchers in the field of LFC have used a variety of optimization techniques, such as Artificial Electric Field Algorithm (AEFA) [20] FOTID controller optimized with Path Finder Algorithm (FPA) [21], Fitness Dependent Optimizer (FDO) [22], Grasshopper Optimization Algorithm (GOA) [23], Firefly Algorithm (FA) [24], Harries Hawks Optimizer (HHO) [25], Frog Leaping Algorithm (FLA) [26], Marine Predator Algorithm (MPA) [27], Imperialist Competitive Algorithm (ICA) [28], Gray Wolf Optimizer (GWO) [29], Sine Cosine Algorithm (SCA) [30], Fuzzy PID controller optimized with Improved Ant Colony Optimization (IACO) [31], Atomic Search Optimization (ASO) [32], Improved Fitness Dependent Optimizer (I-FDO)

[33], Hybrid PSO based Gravitational Search Optimization (GSO) [34], Volleyball Premier League (VPL) based optimized fractional order control [35], Hybrid Differential Evolution (DE) with Pattern Search (PS) algorithm [44], Hybrid Teaching-Learning Optimization with PS [36], Water Cycle Algorithm (WCA) based optimized I-TD controller [37], Gorilla Troops Optimizer [38] and Salp Swarm Algorithm (SSA) [39] algorithm. However, most of the above algorithms have the drawbacks of parametric sensitivity, premature convergence, and complex computation. To overcome these shortcomings, a new intelligent controller named FOI-TDN controller is presented in this work, along with a new meta-heuristic approach of hybrid SC with FDO algorithm. The main advantage of SC is the high exploitability of the search space. Incorporating the features of SC to refine the search for best neighbors and FDO to explore the entire search space for possible solutions leads to an improvement in the exploitability of FDO. For a comprehensive understanding of the LFC problem, it is crucial to include the important inherent requirements as well as the basic physical constraints in the model. In this regard, most authors have considered only a few constraints such as GRC and GDZ and neglected all possible practical constraints. However, in this study, all physical constraints such as GRC, GDZ, CTD, and BD are considered for the LFC problem of two area multi-generation resources like hydro, wind, and reheat thermal systems. Flexible AC Transmission Systems (FACTS) have been widely accepted as a way to use power electronic strategies for PS control and operation. Therefore, a TCPS and a CES are proposed in this work to improve the dynamic performance and stability of the system.

B. PREVIOUS WORK'S MOTIVATIONS AND LIMITATIONS
The primary observation based on previous literature is that LFC strategies that rely on the controller designer's experience, such as MPC, fuzzy logic control, and H-infinity techniques, achieve the desired performance but have some design flaws and take a long time to select control parameters. In addition, conventional PI and PID controllers have difficulties in dealing with system uncertainties. Most previous research paid little attention to many robustness analyses (e.g., system nonlinearities, system deficiencies, and system parameter variations). In addition, most previous research did not investigate the effect of a high renewable energy penetration on changes in system parameters. Based on these facts, this work proposes a new updated structure for the FOTIDN controller, called FOI-TDN controller, to improve the system frequency stability in the presence of system uncertainties, nonlinearities, and numerous load disturbances. In addition, the characteristics of the proposed FOI-TDN controller were chosen in accordance with the hSC-FDO to maintain both frequency and system stability under abnormal conditions.

C. CONTRIBUTION AND ORGANIZATION OF PAPER
In this study, the frequency stability of a two-area interconnected multi-source power system integrated with high renewable penetration is considered. A modified structure of the FOTIDN controller, called FOI-TDN controller, is used, which takes into account system uncertainties, nonlinearities and different load patterns. The main contribution of the research is summarized as follows compared to recent works on similar topics:

1) Design and implement a modified version of the FOTID controller known as FOI-TD controller with filter derivative for two areas, six-generation units interconnected PS including all practical constraint like GRC, GDZ, CTD and BD.
2) The proposed controller is optimized using a new meta-heuristic approach of hybrid SC with FDO algorithm.
3) This study compares the performance of the proposed hybrid SC-FDO algorithm with benchmark methods such as FDO, PSO and FA, to demonstrate its effectiveness.
4) The efficiency of the FOI-TDN controller is also compared with that of benchmark controllers such as FOTID, PID, and FOPID.
5) Further TCPS and CES are proposed in this study to improve the dynamic performance and stability of the system.
6) Furthermore, a sensitivity analysis is performed to show the potency of the proposed FOI-TDN controller by altering the system parameters and load conditions.

The rest of this paper is laid out as follows. Section II describes the model of the power system under investigation followed by modeling of TCSP and CES. Section III discusses the proposed FOI-TDN controller configuration, the proposed optimization technique, and the suggested controller design procedures. Section IV contains the simulation results and analysis. Finally, in Section V, the conclusion and future work is presented.

II. POWER SYSTEM MODEL
The system under this research is a two-area distributed generation system consisting of reheat-thermal,, and wind turbines interconnected by a transmission line, as shown in Fig. 1. Moreover, practical constraints such as GRC, CTD, GDZ, and BD are incorporated into two interconnected domains PS with the addition of TCPS and CES to improve the stability of the system. The nonlinear constraints such as GRC are considered for hydrothermal units. For a thermal unit, a GRC of 10% per minute is used for both drawdown and uplift; for a hydro unit, the GRC is 360% per minute for drawdown and 270% per minute for uplift [39]. Nevertheless, communication time delays (CTDs) are another set of inherited practical constraints that have a significant impact on the current power system. The interconnected system utilises a large number of measurement and sensor devices that are normally located at remote sites. The control centre receives data from the metering devices to generate the proper control signal, which is relayed from the control centre to the

generating units for appropriate response. The transmission and reception of signals between different units may not be fast; this delay is called CTD. Due to these CTDs, there is an interruption in changing the PS operating point, which has a significant impact and can occasionally cause the system to become unstable [33].

To overcome the aforementioned problem, CTDs must be included in the LFC study. A boiler is considered an integral part of any thermal plant that produces steam under pressure. Normally, boilers are drum boilers, also known as circulating boilers. The energy given off by the hot furnace walls (also known as water walls) is absorbed by the drum fluids through natural or forced circulation. The boiler receives preheated feed water from the economizer and uses it to produce saturated exhaust steam. This covers the long-standing effects of fuel and steam flow dynamics on the pressure in the boiler drum.

The present study considers BD in coal-fired units with well-tuned controls while analyzing the performance of LFC. Fig 2 depicts the block diagram representation of BD. The TF model for BD can be written as [9].

$$T_{cpu}(s) = \frac{(1 + sT_{1B})(1 + sT_{RB})K_{1B}}{(1 + 0.1sT_{RB})s} \quad (1)$$

$$T_{fs} = \frac{e^{-t_d s}}{1 + sT} \quad (2)$$

Additionally, this work considers the practical constraint GDZ solely for thermal and hydro units. GDZ is limited to 0.05 % in thermal units and 0.02 % in hydroelectric units. The TF for GDZ is given below [22]:

$$GDB = \frac{0.8 - \frac{0.2\Pi}{s}}{1 + sT} \quad (3)$$

A. CAPACITIVE ENERGY STORAGE (CES)

Electrical energy can be stored and released in huge quantities using capacitive energy storage (CES). CES devices are fascinating consideration in theoretical and experimental research for their enormous potential in modern PS applications. They may be used to regulate system frequency variations caused by system transients and to mitigate low-frequency power fluctuations. Numerous advantages of CES include a rapid charge/discharge rate without sacrificing efficiency, a shorter response time, an increased power density, a longer service life, a large capacity for supplying high/ intermittent energy demand to the grid, no maintenance requirements, an environmentally friendly design, and simple and low-cost operation [40]. The CES unit consists of a capacitor, a power conversion system (PCS), and associated protection circuits. Under normal working conditions, the CES unit stores energy and immediately releases it to the grid through the PCS when a sudden load demand occurs. Thus, the CES unit assists AGC in quickly regulating PS to the final equilibrium state. The CES unit has an energy efficiency of about 95% [41]. Certain losses occur due to the energy conversion mechanism, internal leakage and self-discharge. To ensure that the dynamic performance of the power system is improved, and to mitigate

variations in frequency and interconnection power, the CES units are included in both regions of the power system models considered. The incremental change in CES unit power is denoted by Eq (4) [41].

$$CES_1 = CES_2 = \Delta F[\frac{K_{CES}}{sT_{CES} + 1}][\frac{sT_1 + 1}{sT_2 + 1}][\frac{sT_3 + 1}{sT_4 + 1}] \quad (4)$$

where T_1, T_2, T_3, and T are the phase adjustment blocks' time constants. K_{CES} signifies the gain, while T_{CES} is the CES unit's time constant and ΔF denotes an area's frequency deviation signal.

B. MODELLING OF THYRISTOR CONTROLLED PHASE SHIFTER (TCPS)

TCPS is a promising FACTS controller that is widely used in contemporary PSs for transmission line series compensation level applications. It is used to increase the capability of a transmission line's power transfer by dampening the power fluctuations caused by local and inter-area fluctuations. The modeling of TCPS is shown in Figure 3. TCPS enhances the power grid's dependability and stability by enabling flexible power planning in a variety of (changing) operating scenarios. The TCPS unit maintains real power flow in tie-lines under adverse environments, relieves high-frequency irregularity, and regulates system voltage by altering their relative phase angles [16].

The additional power flow between the area-1 and area-2 tie-lines can be indicated by Eq (5) [16].

$$\Delta P_{tie12}(S) = \frac{[\Delta F_1(s) - \Delta F_2(s)]2\pi T_{12}}{S} \quad (5)$$

After inserting a TCPS component into the proposed model, the actual power interchange between areas 1 and 2 through tie-line can be stated as follows [16]

$$\Delta P_{tie12}^{Actual} = \frac{|V_1||V_2|}{X_{12}}[\sin(\sigma_1 - \sigma_2 - \Phi)] \quad (6)$$

The perturbation in the power flow between the tie lines, as illustrated by Eq (7).

$$\Delta P_{tie12}^{Actual} = T_{12}[(\Delta\sigma_1 - \Delta\sigma_2)](T_{12}\Delta\Phi) \quad (7)$$

where

$$T_{12} = \frac{|V_1||V_2|}{X_{12}}[\cos(\sigma_1 - \sigma_2 - \Phi)] \quad (8)$$

Additionally, we know that angular deviation can be expressed as

$$\Delta\sigma_1 = 2\pi \int \Delta F_1 dt, \quad \text{and} \quad \Delta\sigma_2 = 2\pi \int \Delta F_2 dt \quad (9)$$

By taking the Laplace Transform of (7), we obtain

$$\Delta P_{tie12}^{Actual}(s) = T_{12}\Delta\Phi(s)\frac{[\Delta F_1(s) - \Delta F_2(s)]2\pi T_{12}}{S} \quad (10)$$

The phase shifter angle ($\Delta\Phi$) adjusts the tie-line power flow exchange and is given as follows.

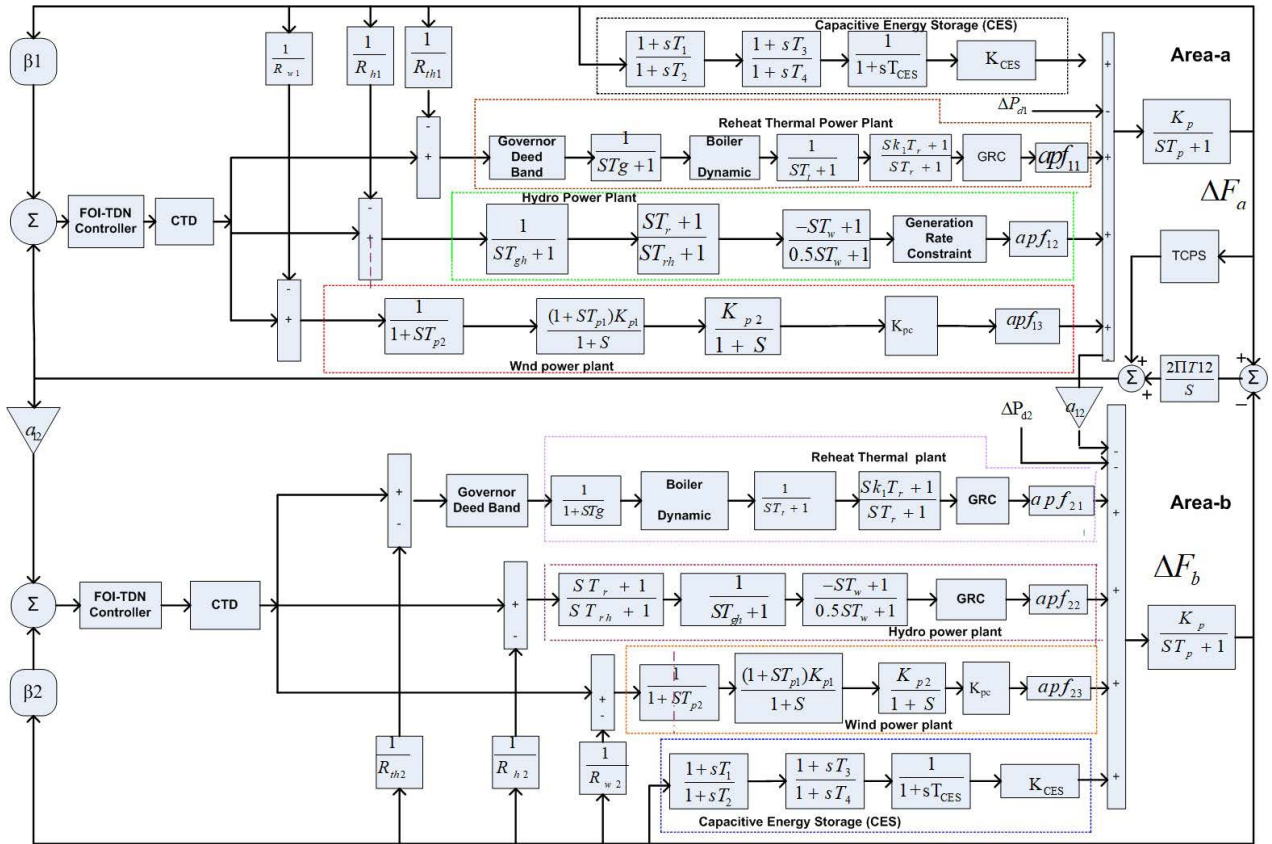$$\Phi(s) = \frac{K_{(\Phi)}}{1 + sT_{TCPS}}[\Delta(Error(s)) \quad (11)$$

FIGURE 1. TF model of two area IPS with multi-unit generations.

where the error signal is the change in frequency, K_Φ shows the stabilization gain, and T_{TCPS} signifies the time constant of the TCPS component. Also Eq (11) can be written as:

$$\Delta P_{tie12}^{Actual} = \Delta F_1(s) - \Delta F_2(s)[\frac{2\pi T_{12}}{S}] + T_{12}\frac{K_{(\Phi)}}{1 + sT_{TCPS}}$$
(12)

III. CONTROLLER STRUCTURE AND OPTIMIZATION TECHNIQUES

Various integer and fractional order controllers are used for LFC in different power systems applications. In the literature, the PID has a wide range of applications in frequency stability difficulties. The PID controller's transfer function is written as follows:

$$TF_{PID}(s) = K_p + \frac{K_i}{S} + K_d(s)$$
(13)

Although the derivative mode of a PID controller enhances system stability and boost controller reaction speed, it results in unreasonably large control inputs to the plant. Large plant input signals result from noise in the control signal, and these problems are common in real-world systems. This problem can be solved by adding a first filter to the derivative term and fine-tuning its pole so that the chattering caused by noise is minimized and its transfer function is given below [33]:

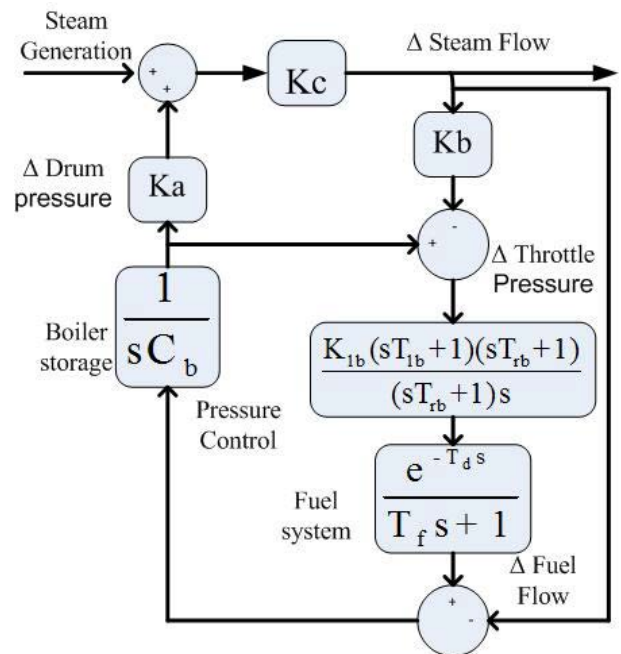$$TF_{PIDN}(s) = K_p + \frac{K_i}{S} + \frac{Ns}{N + s}K_d(s)$$
(14)

FIGURE 2. TF model of boiler dynamic.

The proportional part of a PIDN controller is replaced by a tilting component with a transfer function of $S^{(\frac{-1}{n})}$ in a TIDN controller. The TIDN controller's output transfer function is closer to an optimal transfer function, resulting in a more
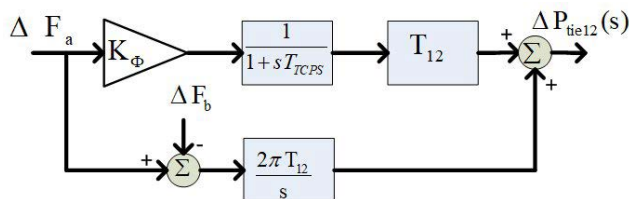
FIGURE 3. Modelling of TCPS.

effective feedback controller.

$$TF_{TIDN}(s) = \frac{K_p}{S^{(\frac{1}{n})}} + \frac{K_i}{S} + \frac{Ns}{N+s}K_d(s) \qquad (15)$$

Surprisingly, despite these benefits, FOI-TD with derivative Filter (FOI-TDN) controller structures are not used for LFC problems. In light of the foregoing, this paper represents the first attempt to apply a FOI-TDN controller to the LFC of an IPS. The FOI-TDN and FOTIDN controllers contain the same amount of parameters but have a different structure, as illustrated in 4 (a) and (b) respectively. Eq (16)) and Eq (17)) represent the transfer function of FOTIDN and FOI-TDN controllers, respectively. The proportional, integral, and differential coefficients of the PID controller, as well as the tilt gain of the proportional component, are expressed by the parameters K_P, K_I, K_D, and K_t of the proposed controller. These gains can be adjusted between $[-5, 5]$. The FO operators μ, λ, on the other hand, can be tuned in the range $[0, 1]$. While n is the tilt fractional component, which can be adjusted between 0 and 10. Similarly, N is the coefficient of the proposed controller's derivative filter, which can be set in the range $[1, 500]$.

$$U(s) = E(s)[\frac{K_p}{S^{(\frac{1}{n})}} + \frac{K_i}{S^\lambda} + \frac{Ns^\mu}{N+s^\mu}K_d(s)] \qquad (16)$$

$$U(s) = E(s)[\frac{K_i}{S^\lambda}] - Y(s)[\frac{K_p}{S^{(\frac{1}{n})}} + \frac{Ns^\mu}{N+s^\mu}K_d(s)] \qquad (17)$$

The objective function is first developed based on the desired requirements and constraints in the formulation of a modern heuristic optimization technique with the controller. In control design, performance criteria such as the integral of time multiplied absolute error, integral of squared error, integral of time multiplied squared error, and the integral of absolute error are frequently taken into account which is given as below respectively:

$$IAE = \int_0^T [|\Delta F_a| + |\Delta F_b| + |\Delta P_{tie}|]dt \qquad (18)$$
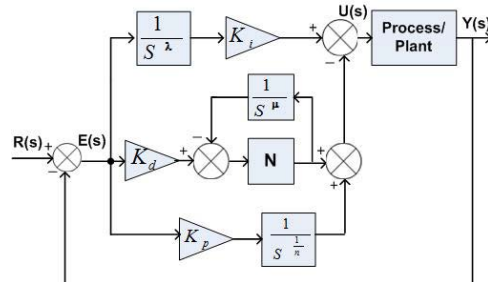
$$ISE = \int_0^T [\Delta F_a^2 + \Delta F_b^2 + \Delta P_{tie}^2]dt \qquad (19)$$

$$ITAE = \int_0^T t[|\Delta F_a| + |\Delta F_b| + |\Delta P_{tie}|] \qquad (20)$$

$$ITSE = \int_0^T t[\Delta F_a^2 + \Delta F_b^2 + \Delta P_{tie}^2]dt \qquad (21)$$
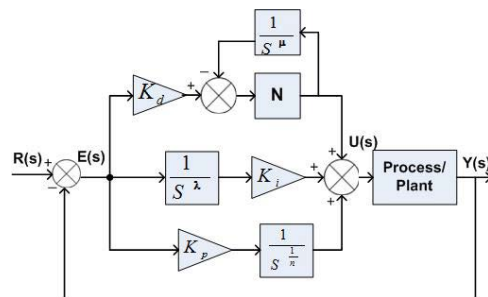
(a)

(b)

FIGURE 4. Structure of controllers (a) FOTIDN Controller (b) FOI-TDN Controller.

A. FITNESS DEPENDENT OPTIMIZER (FDO)

The FDO [42] has a unique approach for calculating velocity (pace). It utilizes a fitness function to generate appropriate weights, which aid the search agents in balancing exploration and exploitation. Using the upper and lower bounds, the FDO method assigns random solutions to the scout bee population. Scout bees use a fusion of a casual walk and a fitness weight manner to find hives. By adding pace to their existing position, the scout bees modify their position. The scout bees' movement is estimated as [42]:

$$X_{k,t+1} = P + X_{k,t} \qquad (22)$$

$X_{k,t+1}$ denote the next location, while $X_{k,t}$ denotes the current location and P represent the pace. The fitness weight (F_w) is calculated according to Eq (30))

$$F_w = |\frac{f(X)_{k,t}^*}{f(X)_k^t}| - \gamma \qquad (23)$$

Furthermore, the following are the necessary conditions for F_w [42].

$$P = RX_k^*t; \text{ if } f(X)_k^t = 0 \text{ or } \gamma = 0 \text{ or } \gamma = 1, \text{ and}$$

$$P = \begin{cases} \gamma(X_k^t - X_{k,t}^*) - 1 & \text{if } 0 < \gamma < 1 \text{ and } R < 0 \\ -\gamma(X_k^t - X_{k,t}^*) & \text{if } < \gamma < 1 \text{ and } R \geq 0 \end{cases} \qquad (24)$$

where R signifies random numbers within the $[-1, 1]$ set.

B. SINE COSINE ALGORITHM (SCA)

The behavior of the sine cosine algorithm (SCA) in attaining best solutions is based on the cosine and sine functions. SCA generates several preliminary arbitrary solutions that vary

towards or away from the best solutions [30]. For sine and cosine phases, the following position updating equations are proposed [30].

$$X_i^{t+1} = X_i^t + r_3|q_i^t X_i^t|r_1 \sin(r_2) \qquad (25)$$

$$X_i^{t+1} = X_i^t + r_3|q_i^t X_{ii}^t|r_1 \cos(r_2) \qquad (26)$$

X_i^{t+1} denote the next location, while X_i^t denotes the current location and q represent the destination points. Where r_1 denotes the next position regions, r_2 specifies how far the movement should be towards or away from the destination and r_3 generates destination weights at random.

$$X_i^{t+1} = \begin{cases} (X_i^t + r_3|q_i^t X_i^t|r_1 \sin(r_2) & \text{if } r_4 < 0.5 \\ X_i^t + r_3|q_i^t X_i^t|r_1 \sin(r_2) & \text{if } r_4 \geq 0.5 \end{cases} \qquad (27)$$

where r_4 is a random number between 0 and 1. As shown in Eq (27)), r_4 alternates between the sine and cosine components.

C. HYBRID SINE COSINE WITH FITNESS DEPENDENT OPTIMIZER (HSC-FDO)

This algorithm was developed by Chan.C by partially integrating the algorithm SC into the FDO techniques to improve the performance of the original FDO in terms of search accuracy, convergence speed, and the balance between exploration and exploitation capabilities in the search space [43]. In this technique, four modifications are employed which is given as below:

1) Modified Pace-Updating Equation: in this section, the notion of improved pace updating is introduced to increase the speed of convergence and the balance of exploration and exploitation capabilities of the original FDO. The equation for modified pace-updating is given below [43]:

$$P = \begin{cases} RX_k^* t; & \text{if } \gamma = 1 \\ X_k^t + (r_1 \cos r_2 r_3 X_{k,t}^* - X_K^t)R; \\ & \text{if } \gamma = 0 \\ (\gamma(X_k^t + (r_1 \sin r_2 r_3 X_{k,t}^* - X_K^*)); \\ & \text{if } 0 < \gamma < 1 \text{ and } R \geq 0 \\ (\gamma(X_k^t + (r_1 \sin r_2 r_3 X_{k,t}^* - X_K^*)) - 1; \\ & \text{if } 0 < \gamma < 1 \text{ and } R < 0 \end{cases} \qquad (28)$$

2) Global Fitness Weight Strategy and Random Weight Factor: a random weight component and a global fitness weight constraint are incorporated into the search process to improve the performance of the proposed SC-search FDO. To increase the convergence and superiority of the solutions, the SC-FDO algorithm includes a modified calculation of the fitness weight Fw, which is given as follows [43]:
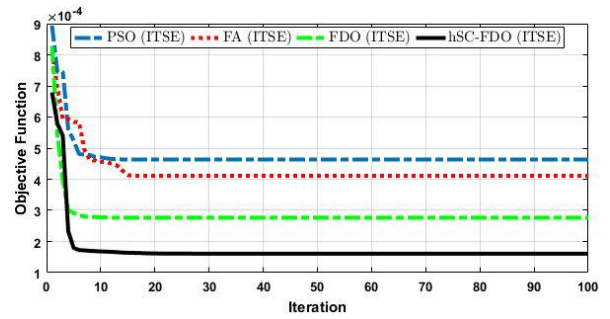
$$F_w = |\frac{f(X)_{k,t}^*}{f(X)_k^t}| \qquad (29)$$

FIGURE 5. Convergence diagram for different algorithms.

TABLE 2. Comparative performance of different performance indices.

Techniques	Performance Indices			
	IAE	*ITAE*	*ISE*	*ITSE*
FOI-TDN (hSC-FDO)	0.0147	0.0006	0.00009	0.00003
FOI-TDN (FDO)	0.0196	0.0023	0.00026	0.00022
FOI-TDN (FA)	0.0293	.0010	0.000270	0.00020
FOI-TDN (PSO)	0.0820	.0098	0.000980	0.00056

3) Conversion Parameter Strategy Parameters: r_1, r_2, and r_3 in the improved pace apprising equation convert search from exploitation to exploration at promising locations. The following solution's region is determined by the parameter r_1, as indicated in Eq (27)). The high r_1 value fosters global exploration, whereas a low r_1 value supports local exploitation in the direction of the destination. But, r_1 is linearly decreased from (a) to (0) to accomplish a balanced exploration and exploitation, and is stated as follows [43]:

$$r_1(t) = [1 - \frac{t}{t_{max}}]\beta \qquad (30)$$

where β represents a constant, t represents the current iteration and t_{max} represents the maximum iteration. The flow scheme for hybrid SC-FDO technique is given in Fig 6.

IV. VALIDATION PERFORMANCES

In this section, a multi-renewable resource with a two-area interconnected system assimilated with CES and TCPS depicted in Fig 1 is developed in Matlab/Simulink environment using Appendix via 1 % step load disturbance (SLD) at t = 0 s. An ITSE-based hybrid SC-FDO technique is employed to optimize the effectiveness of the newly developed FOI-TDN controller. The ITSE base suggested algorithm is favored due to its superior cost function values, as shown in Table 1. After 30 iterations and selecting the optimum values, the parameters of the hSC-FDO listed in Appendix are used to calculate the proposed controller's optimal gains, which are listed in Table 3. The performance of the LFC system of two area multi-generation units has been validated with respect to three scenarios in order to demonstrate its performance.

1) **Scenario-1 (FOI-TDN based different algorithms)**
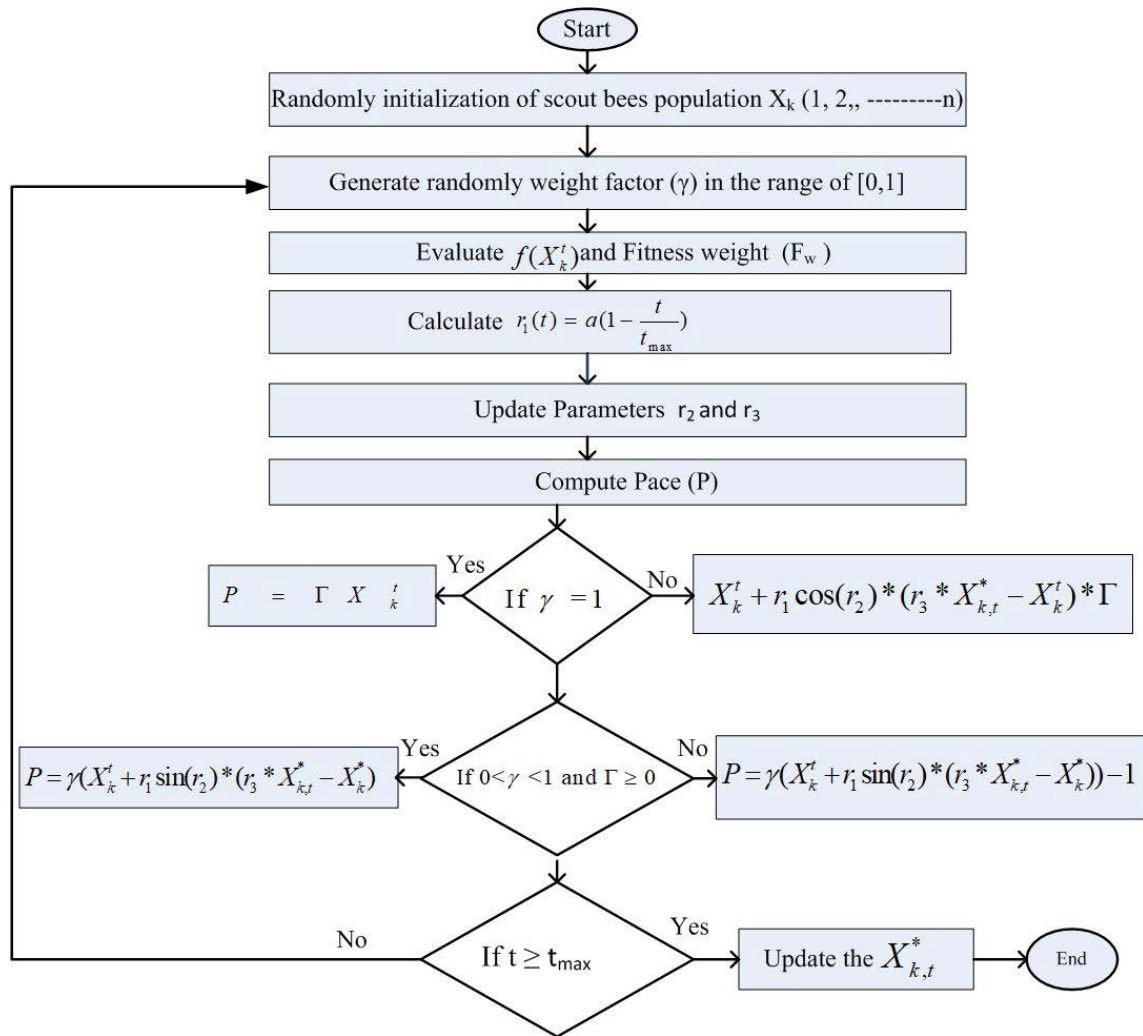   In this case, the hSCA-FDO meta-heuristic algorithm

FIGURE 6. Flow chart of hSC-FDO Algorithm.

TABLE 3. Parameters setting considering various scenarios.

Controller Parameters	Scenario-1(FOI-TDN)				Scenario-2 (hSC-FDO)			
	hSC-FDO	FDO	FA	PSO	PID	FOPID	FOTID	FOI-TDN
K_{p1}	1.130	1.091	1.010	1.176	1.290	1.405	1.032	0.998
K_{i1}	0.200	1.012	0.305	1.232	0.232	1.012	1.024	1.010
K_{d1}	1.030	-1.023	0.011	1.190	0.010	1.890	0.110	1.900
$\lambda 1$	0.765	0.789	0.991	1.223	-	0.343	0.786	0.334
n_1	0.765	0.789	0.245	0.230	-	-	0.786	0.445
$\mu 1$	0.003	0.675	0.910	1.347	-	0.989	0.567	-0.445
N_1	3.003	9.675	7.910	6.002	-	-	-	9.345
K_{p2}	1.012	0.305	1.232	0.305	0.200	0.232	1.012	1.983
K_{i2}	1.023	0.011	1.190	0.011	1.030	0.010	1.890	0.110
K_{d2}	1.030	-1.023	0.011	1.190	0.010	1.890	0.110	1.900
$\lambda 2$	0.765	0.006	0.890	0.015	-	0.113	0.234	0.878
n_2	0.013	0.124	0.102	0.013	-	-	0.234	0.656
$\mu 2$	0.675	0.910	0.002	0.345	-	0.900	0.344	0.236
N_2	3.091	9.010	10.176	21.290	-	-	-	10.567

is compared to benchmark methodologies such as FDO, PSO, and FA to demonstrate the effectiveness of our suggested model. Fig 5 illustrates the convergence curve for various methods, revealing that our suggested hSC-FDO algorithm converges faster than

FDO, PSO, and FA. Different performance indices are calculated for the various algorithms under consideration, as shown in Table 2. The comparison contains values for the ISE, IAE, ITSE, and ITAE meta-heuristic algorithms. Table 2 demonstrates that the suggested
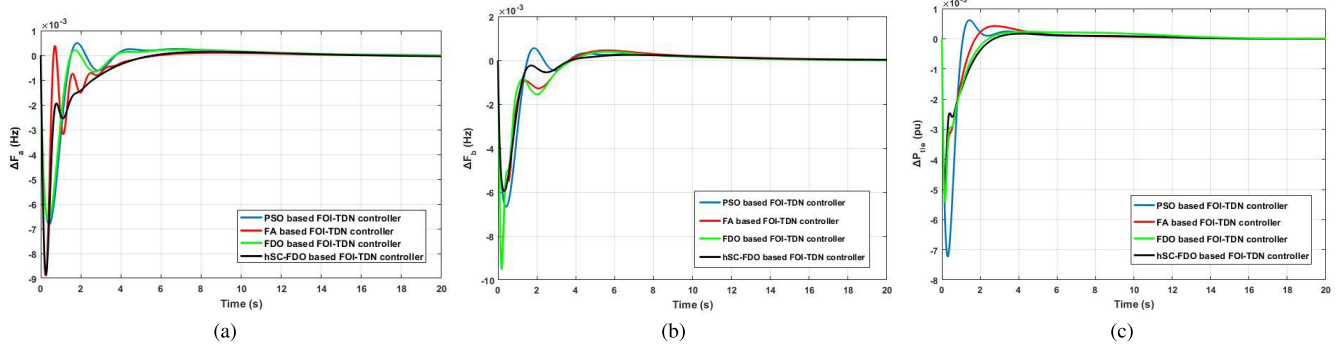
FIGURE 7. Response of the system considering scenario-1 for (a) ΔF_a; (b) ΔF_b; (c) ΔP_{tie}.

approach outperforms competing algorithms in terms of all calculated performance indices. Additionally, the evaluated performance indices demonstrate the suggested techniques' superiority to alternative algorithms. The ITSE values are 0.00022, 0.00020 and 0.00022 for the PSO, FA, and FDO algorithms, respectively. Similarly, the ISE values are 0.00098, 0.00027 and 0.00026 for the PSO, FA, and FDO algorithms, respectively. Furthermore, the ITAE values are 0.0097, 0.0010 and 0.0023 for PSO, FA, and FDO algorithms, respectively. Whereas, the IAE values are 0.0820, 0.0293 and 0.0196 for PSO, FA, and FDO algorithms, respectively. To summarize, the proposed algorithms for hSCA-FDO controllers obtain the highest performance indices when compared to other algorithms addressing the same controllers. The dynamic transient response of an AGC system is illustrated in Fig 7 (a–c) using various methodologies for frequency deviation in area-a (ΔF_a), area-b (ΔF_b), and tie-line power deviations (ΔP_{tie}). As illustrated in Fig 7 (a–c), the FOI-TDN controllers based on hSCA-FDO optimization rapidly suppressed oscillation and reduced peak overshoot and undershoot for ΔF_a, ΔF_b, and ΔP_{tie}. Table 4 shows a detailed comparison of the results for ΔF_a, ΔF_b, and ΔP_{tie} for various methods in terms of Overshoot (Os), Undershoot (Us), and Settling time (Ts). In comparison to a FOI-TDN based PSO algorithms, hSC-FDO tuned FOI-TDN controller improved settlement time by 49.45%, 1.38%, and 4.53%, and effectively reduced overshoot by 87.21%, 49.71 %, and 10.56 % for ΔF_a, ΔF_b, and ΔP_{tie}. Table 3 shows that when compared to the Pathfinder algorithm-based FOTID controller, the hSC-FDO-based tuned FOI-TDN controller offers a significant increase of 78.43%, 37.10 %, and 83.89 % effectively reducing peak overshoot of 86.53%, 49.34%, and 87.33 % and undershoot of 35.45 %, 59.48 %, and 49.22 % for two areas and in tie-line power. In comparison to the WCA-based I-TD controller, the FOI-TDN based hSC-FDO controller improves time settling by 35.98%, 72.41%, and 14.11 % for ΔF_a, ΔF_b, and ΔP_{tie} respectively.

2) **Scenario-2 (CES and TCPS)** The effect of introducing CES and TCPS units on LFC is investigated in scenario-2. Each area has a CES unit, and the system's tie-line takes TCPS into account. The system's performance is assessed using hSC-FDO-based FOI-TDN controller with the effects of CES, TCPS, both CES and TCPS, and without CES and TCPS. Fig 8(a-c) depicts the results obtained for ΔF_a, ΔF_b, and ΔP_{tie} respectively which reveals the superior performances of the hSC-FDO based CES and TCPS model in terms of Os, Ts, and Us. When it is compared with a system that does not have the effect of the CES and TCPS unit, the system's dynamic response with TCPS and CES unit improves in terms of settling time (19.21%, 22.86 %, and 31.98%), overshoot (45.23%, 71.10 %, and 56.13%), and undershoot (39.88 %, 19.28 %, and 19.96 %) ΔF_a, ΔF_b, and ΔP_{tie} respectively. The system's response to TCPS and CES unit consequences are better in terms of Os, Ts, and Us when compared to the system's response without TCPS and CES unit effects for ΔF_a, ΔF_b, and ΔP_{tie} respectively as shown in Fig 8(a-c). Furthermore, Table 5 shows that our proposed approach performs admirably when combined with CES and TCPS.

3) **Scenario-3 (hSC-FDO based various controllers)** In this scenario, the performance of FOI-TDN controller tuned with hSc-FDO algorithm was compared to FOTID, FOPID, and PID controllers optimized with the similar methodology. Fig 9(a-c) and Table 6 demonstrate the findings achieved using the recommended strategies. Table 5 shows that the FOI-TDN controller tuned with hSC-FDO approach outperforms the FOPID controller with hSC-FDO techniques in terms of settling time (9.75 %, 23.33 %, and 32.12 %) and overshoot (72.63 %, 89.77 %, and 87.34 %) for ΔF_a, ΔF_b, and ΔP_{tie}, respectively. As for comparison with PID controller that is tuned with alike algorithms, FOI-TDN controller improved settling time by (44.22 %, 12.53 %, and 32.56 %), effectively compact peak overshoot by (51.22 %, 85.22 %, and 79.11 %), and reduced undershoot by (32.67 %, 54.34 %, and 79.30 %) for ΔF_a, ΔF_b, and ΔP_{tie}, respectively. Conclusively,

TABLE 4. Comparative analysis of various algorithms considering case-1.

Controller with Techniques	Settling Time $T_s s$			Undershoot U_{sh}			Overshoot O_{sh}		
	ΔF_a	ΔF_b	ΔP_{tie}	ΔF_a	ΔF_b	ΔP_{tie}	ΔF_a	ΔF_b	ΔP_{tie}
FOI-TDN (PSO)	13.30	12.8	12.2	−0.0068	−0.0066	−0.0073	0.00049	0.00055	0.00110
FOI-TDN (FA)	11.60	13.4	9.10	−0.0089	−0.0093	−0.0049	0.00090	0.00094	0.00017
FOI-TDN (FDO)	13.15	11.6	8.72	−0.0066	−0.0095	−0.0053	0.00022	0.00029	0.00043
FOI-TDN(hSC-FDO)	10.13	11.4	8.60	−0.0088	−0.0059	−0.0049	0.00014	0.00024	0.00610
TID (hTLBO-PS) [36]	9.53	13.75	10.36	−0.18888	−0.24010	−0.06330	0.007222	0.070400	0.003500
MID (hDE-PS) [44]	19.07	18.09	12.69	−0.00100	−0.01500	−0.00800	0.00080	0.001700	0.000600
FPA-OTID [21]	25.59	23.25	18.77	−0.02450	−0.0228	−0.0044	0.00680	0.01170	0.00260
WCA-I-TD [37]	12.29	29.45	30.50	−0.0109	−0.0035	−0.0022	0.00280	0.00110	0.00700

TABLE 5. Comparative performance for scenario-2.

Controller with Techniques	Settling Time $T_s s$			Undershoot U_{sh}			Overshoot O_{sh}		
	ΔF_a	ΔF_b	ΔP_{tie}	ΔF_a	ΔF_b	ΔP_{tie}	ΔF_a	ΔF_b	ΔP_{tie}
FhSC-FDO without TCPS and CES	12.1	11.8	12.4	−0.00823	−0.01023	−0.00695	0.00363	0.001410	0.001641
hSC-FDO with CES	11.8	9.90	8.20	−0.00812	−0.00691	−0.00568	0.00224	0.000557	0.000319
hSC-FDO with TCPS	11.2	9.80	7.80	−0.00685	−0.00912	−0.00441	0.00223	0.000508	0.000318
hSC-FDO with TCPS and CES	10.8	8.10	6.23	−0.00681	−0.00446	−0.00527	0.00116	0.000115	0.000039

TABLE 6. Comparative performance for scenario-3.

Controller with Techniques	Settling Time $T_s s$			Undershoot U_{sh}			Overshoot O_{sh}		
	ΔF_a	ΔF_b	ΔP_{tie}	ΔF_a	ΔF_b	ΔP_{tie}	ΔF_a	ΔF_b	ΔP_{tie}
hSC-FDO with PID	18.1	19.2	15.36	−0.00111	−0.00149	−0.00053	0.000225	0.000409	0.000060
hSC-FDO with FOPID	19.9	19.4	14.47	-0.00098	−0.00137	−0.00052	0.000151	0.000153	0.000028
hSC-FDO with FOTID	19.4	18.2	13.30	−0.00080	−0.00117	−0.00049	0.000168	0.000174	0.000021
hSC-FDO with FOI-TDN	18.3	17.6	13.80	−0.00060	−0.00410	−0.00097	0.000085	0.000044	0.000000
TID (hTBO-PS) [36]	26.17	27.99	18.78	−0.42160	−0.39500	−0.07590	0.05910	0.0599	0.039000
MID (hDE-PS) [44]	18.58	20.15	19.05	−0.00150	−0.00100	−0.01890	0.001600	0.0010	0.001000
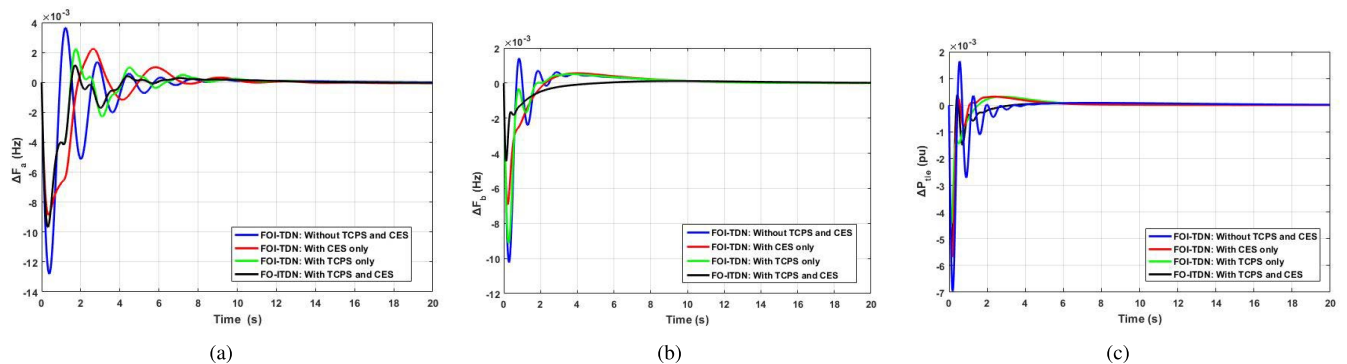
FIGURE 8. Response of the system considering scenario-2 for (a) ΔF_a; (b) ΔF_b; (c) ΔP_{tie}.
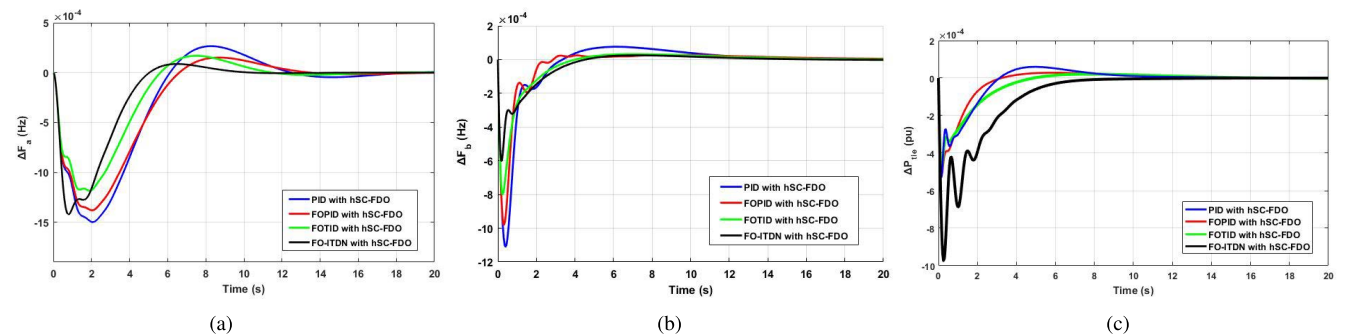
FIGURE 9. Response of the system considering scenario-2 for (a) ΔF_a; (b) ΔF_b; (c) ΔP_{tie}.

it can be observed that our developed controller outperforms PID algorithms and FOPID controllers tuned with hSC-FDO algorithms in terms of O_{sh}, T_s and U_{sh}.

The two-area power system is depicted in 11 (a-c) for various load fluctuation considering area 1, area 2 and tie-line power. The frequency fluctuation is evaluated at different loads and the mitigating ability of controllers is analyzed,
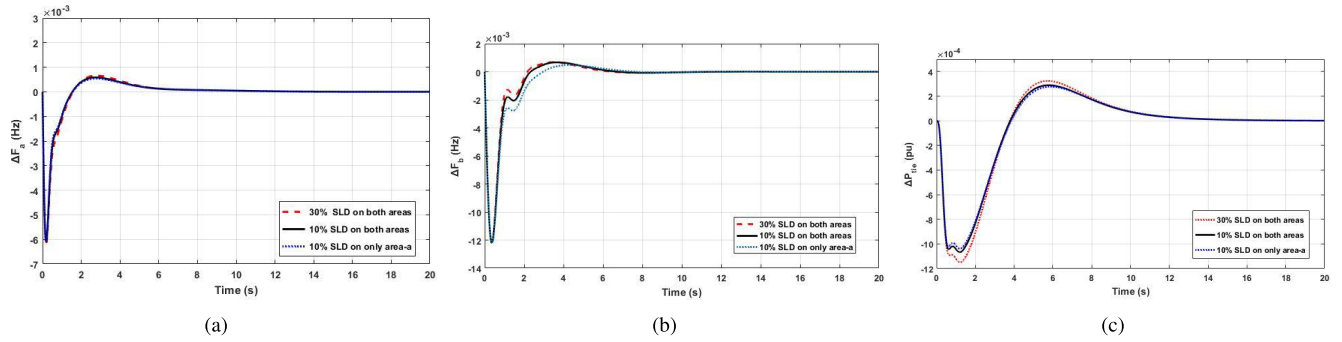
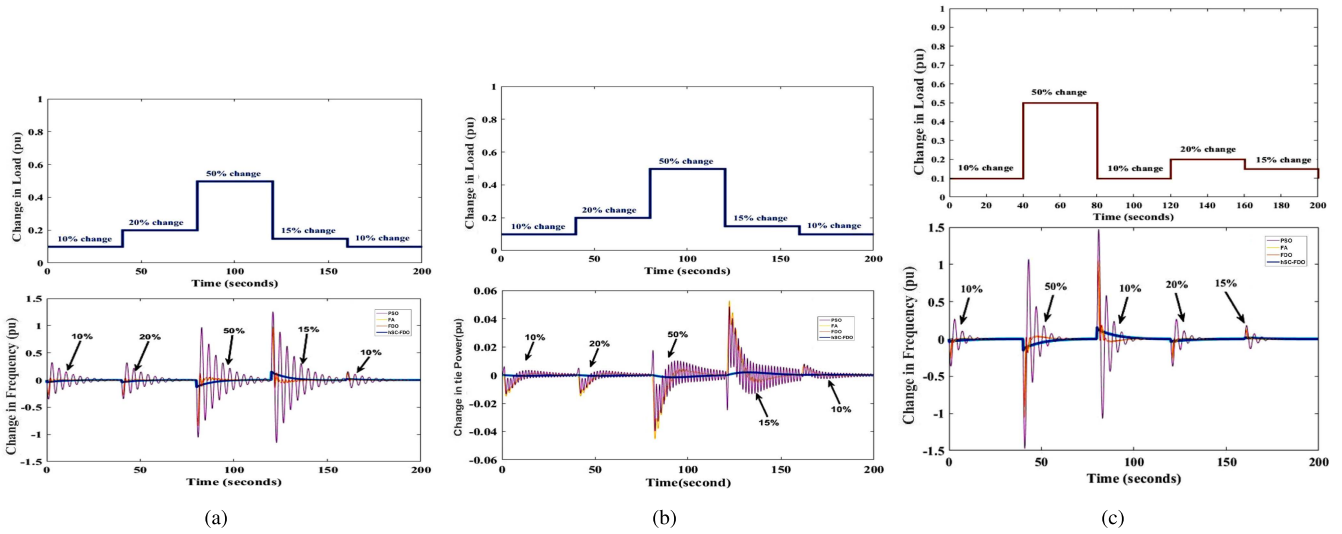**FIGURE 10.** Response of the system considering scenario-2 for (a) ΔF_a; (b) ΔF_b; (c) ΔP_{tie}.

FIGURE 11. Frequency variation with different load conditions for (a) ΔF_a; (b) ΔF_b; (c) ΔP_{tie}.

TABLE 7. Sensitivity analysis for proposed hSC-FDO based FOI-TDN controller.

Controller with Techniques	Settling Time $T_s s$			Undershoot U_{sh}			Overshoot O_{sh}		
	ΔF_a	ΔF_b	ΔP_{tie}	ΔF_a	ΔF_b	ΔP_{tie}	ΔF_a	ΔF_b	ΔP_{tie}
T_g +30%	15.1	12.9	13.9	−0.01056	−0.00682	−0.00916	0.000588	0.000554	0.00274
−30%	12.6	7.6	12.6	−0.00142	−0.00213	−0.01520	0.000086	0.000003	0.00172
R +30%	15.2	17.6	17.7	−0.01056	−0.00824	−0.00707	0.00117	0.004030	0.004740
−30%	17.6	13.0	17.6	−0.00150	−0.00428	−0.01960	0.00022	0.000136	0.00742
T_w +30%	14.7	17.4	16.9	−0.01085	−0.00813	−0.01190	0.000721	0.00319	0.00444
−30%	15.1	12.9	15.1	−0.00138	−0.00360	−0.01810	0.000152	0.000000	0.00430
T_t +30%	14.8	12.7	15.4	−0.01056	−0.00686	−0.01190	0.000873	0.000660	0.00336
−30%	13.9	8.2	13.9	−0.00118	−0.00258	−0.01520	0.000169	0.000022	0.00263

where hSC-FDO based FOI-TDN reveals its superiority in dealing with quick variations in load as compared to Other techniques, such as FDO, FA, and PSO which exhibit more oscillations.

A. SENSITIVITY ANALYSIS

A robustness analysis is required to evaluate the ability of the LFC controller to withstand uncertainty. In the test, the newly developed system including numerous constraints using the hSC-FDO approach and under the supervision of the controller FOI-TDN was targeted with various loadings such as 10% SLD on area-a only, 10% and 30% SLD on both areas. The responses for this test are shown in

Fig 10(a-c) and indicate that the current control approach can handle the system performs well even under uncertain load. In addition, a sensitivity analysis of the system is also performed by varying the system parameters in a range of $\pm 30\%$ such as the wind time constant (T_w), droop constant (R), the governor constant (T_g), and the turbine constant (T_t). Table 7 shows a comparative study of various parameters in terms of undershooting, overshoot, and settling time with a change of ± 30 % from the nominal values. Thus, even if the system load and parameters vary greatly, there is no need to change the parameters of the FOI-TDN controller. Therefore, the control technique presented here is robust.

V. CONCLUSION AND FUTURE WORK

This study designs and develops a FOI-TDN controller for the LFC of two areas, i.e., six-gen units with the inclusion of practical constraints such as the governor dead zone, communication time delay, boiler dynamics, and generation rate constraint. To tune the gains of the proposed controller, the hSC-FDO meta-heuristic algorithm is used. Moreover, the integration of CES in each area and TCPS in series with the interconnects improves the dynamic response of the system. Based on the simulation results, it was found that the tuned FOI-TDN controller based on hSC-FDO effectively reduces the overshoot (O_{sh}) by 49.31 %, the temporal control by 33.22 % and undershoot (U_{sh}) reduced by 29.13 %, 39.34 % and 56.90 % for the ΔF_a, ΔF_b, and ΔP_{tie} respectively, compared to the hSC-FDO tuned PID controller. Similarly, the HSC-FDO algorithm tuned controller (FOI-TDN) provides a significant improvement in the settling time for both the areas and tie-line power. It also effectively reduces the peak overshoots of 88.90 %, 78.33 %, and 49.13 % and the undershoots of 17.02 %, 69.67 %, and 83.10 % for ΔF_a, ΔF_b, and ΔP_{tie}, respectively, compared to the WCA-based tuned I- TD controller. Moreover, the dynamic response of the system is improved by including the effects of TCPS and CES in terms of Os, Ts, and Us, compared to not including the effects of TCPS and CES for ΔF_a, ΔF_b, and ΔP_{tie}. Finally, for the LFC problem, the capability of the designed FOI-TDN controller was tested by adjusting the system characteristics and load conditions in a range of ±30%. In the future, the research could be extended to modern networked realistic power system using more advanced optimization approaches.

APPENDIX

TABLE 8. Parameter and value of two-area IPS [9].

Parameters	Values	Parameters	Values
β_1,β_2	0.431 MW/Hz	T_{gh}	0.080 s
$R_{th1}, R_{th2}, R_{hy1}$	2.40 Hz/p.u	T_{gh}	0.080 s
R_{hy2}, R_{g1}, R_{g2}	2.40 Hz/p.u	T_t	0.30 s
K_1	0.30	T_r	10 s
K_P	68.95	T_p	11.490 s
T_{12}	0.0430	T_{rh}	28.70 s
a_{12}	−1	T_w	1 s
T_{rs}	5 s	y_c	1 s
T_{gh}	0.60 s	x_c	0.60 s
K_g	0.1304	K_{DC}	1
x_g	1	b_g	0.050 s
K_t	0.5434	T_F	0.230 s
K_h	0.3268	T_{cr}	0.010 s

TABLE 9. Parameters and values of hSC-FDO.

Parameters	Values	Parameters	Values
Population No N_P	30	Generation No N_g	60
Lower bound L_b	−2	Upper bound U_b	2
No of Dimensions N_d	15	Weight Factor γ	[−0, 1]
random number R	[−1, 1]	β	2

ACKNOWLEDGMENT

REFERENCES

[1] Z.-X. Yu, M.-S. Li, Y.-P. Xu, S. Aslam, and Y.-K. Li, "Techno-economic planning and operation of the microgrid considering real-time pricing demand response program," *Energies*, vol. 14, no. 15, p. 4597, Jul. 2021.

[2] K. Ullah, A. Basit, Z. Ullah, S. Aslam, and H. Herodotou, "Automatic generation control strategies in conventional and modern power systems: A comprehensive overview," *Energies*, vol. 14, no. 9, p. 2376, Apr. 2021.

[3] M. Khamies, G. Magdy, M. E. Hussein, F. A. Banakhr, and S. Kamel, "An efficient control strategy for enhancing frequency stability of multi-area power system considering high wind energy penetration," *IEEE Access*, vol. 8, pp. 140062–140078, 2020.

[4] A. Daraz, S. A. Malik, A. Waseem, A. T. Azar, I. U. Haq, Z. Ullah, and S. Aslam, "Automatic generation control of multi-source interconnected power system using FOI-TD controller," *Energies*, vol. 14, no. 18, p. 5867, Sep. 2021. [Online]. Available: https://www.mdpi.com/1996-1073/14/18/5867

[5] Y. Arya, "Improvement in automatic generation control of two-area electric power systems via a new fuzzy aided optimal PIDN-FOI controller," *ISA Trans.*, vol. 80, pp. 475–490, Sep. 2018.

[6] M. K. Debnat, N. C. Patel, and R. K. Mallick, "Optimal base PD-PID controller for automatic generation control of multi-source tuned by teaching learning base optimization algorithm," in *Proc. 7th India Int. Conf. Power Electron. (IICPE)*, Punjab, India, Nov. 2016, pp. 1–6.

[7] M. Khamies, G. Magdy, M. Ebeed, and S. Kamel, "A robust PID controller based on linear quadratic Gaussian approach for improving frequency stability of power systems considering renewables," *ISA Trans.*, vol. 117, pp. 118–138, Nov. 2021.

[8] D. Guha, P. K. Roy, and S. Banerjee, "Disturbance observer aided optimised fractional-order three-degree-of-freedom tilt-integral-derivative controller for load frequency control of power systems," *IET Gener., Transmiss. Distrib.*, vol. 15, no. 4, pp. 716–736, Feb. 2021.

[9] A. Daraz, S. A. Malik, I. U. Haq, K. B. Khan, G. F. Laghari, and F. Zafar, "Modified PID controller for automatic generation control of multi-source interconnected power system using fitness dependent optimizer algorithm," *PLoS ONE*, vol. 15, no. 11, Nov. 2020, Art. no. e0242428, doi: 10.1371/journal.pone.0242428.

[10] Y. Arya and N. Kumar, "BFOA-scaled fractional order fuzzy PID controller applied to AGC of multi-area multi-source electric power generating systems," *Swarm Evol. Comput.*, vol. 32, pp. 202–218, Feb. 2017.

[11] A. Fathy and A. M. Kassem, "Antlion optimizer-ANFIS load frequency control for multi-interconnected plants comprising photovoltaic and wind turbine," *ISA Trans.*, vol. 87, pp. 282–296, Apr. 2019.

[12] E. A. Mohamed, E. M. Ahmed, A. Elmelegi, M. Aly, O. Elbaksawi, and A.-A. A. Mohamed, "An optimized hybrid fractional order controller for frequency regulation in multi-area power systems," *IEEE Access*, vol. 8, pp. 213899–213915, 2020.

[13] A. Elmelegi, E. A. Mohamed, M. Aly, E. M. Ahmed, A.-A.-A. Mohamed, and O. Elbaksawi, "Optimized tilt fractional order cooperative controllers for preserving frequency stability in renewable energy-based power systems," *IEEE Access*, vol. 9, pp. 8261–8277, 2021.

[14] M. Ahmed, G. Magdy, M. Khamies, and S. Kamel, "Modified TID controller for load frequency control of a two-area interconnected diverse-unit power system," *Int. J. Electr. Power Energy Syst.*, vol. 135, Feb. 2022, Art. no. 107528. [Online]. Available: https://www.sciencedirect.com/science/article/pii/S0142061521007651

[15] M. Bhuyan, D. C. Das, and A. K. Barik, "Proficient power control strategy for combined solar gas turbine-wind turbine generator-biodiesel generator based two area interconnected microgrid employed with DC link using Harris's hawk optimization optimised tilt-integral-derivative controller," *Int. J. Numer. Model., Electron. Netw., Devices Fields*, pp. 1–26, Feb. 2022. [Online]. Available: https://onlinelibrary.wiley.com/doi/abs/10.1002/jnm.2991

[16] J. Morsali, K. Zare, and M. Tarafdar Hagh, "Comparative performance evaluation of fractional order controllers in LFC of two-area diverse-unit power system with considering GDB and GRC effects," *J. Electr. Syst. Inf. Technol.*, vol. 5, no. 3, pp. 708–722, Dec. 2018. [Online]. Available: https://www.sciencedirect.com/science/article/pii/S2314717217300211

[17] A. Saha and L. C. Saikia, "Load frequency control of a wind-thermal-split shaft gas turbine-based restructured power system integrating FACTS and energy storage devices," *Int. Trans. Electr. Energy Syst.*, vol. 29, no. 3, p. e2756, Mar. 2019, doi: 10.1002/etep.2756.

[18] Y. Arya, "AGC of PV-thermal and hydro-thermal power systems using CES and a new multi-stage FPIDF-(1+PI) controller," *Renew. Energy*, vol. 134, pp. 796–806, Apr. 2019.

[19] Y. Arya, "A novel CFFOPI-FOPID controller for AGC performance enhancement of single and multi-area electric power systems," *ISA Trans.*, vol. 100, pp. 126–135, May 2020.

[20] C. Naga Sai Kalyan and G. Sambasiva Rao, "Coordinated smes and tcsc damping controller for load frequency control of multi area power system with diverse sources," *Int. J. Electr. Eng. Informat.*, vol. 12, no. 4, pp. 747–769, 2020.

[21] S. K. R. Priyadarshani, Subhashini and J. K. Satapathy, "Pathfinder algorithm optimized fractional order tilt-integral-derivative (fotid) controller for automatic generation control of multi-source power system," *Microsyst. Technol.*, vol. 27, no. 1, pp. 23–35, 2020.

[22] A. Daraz, S. Abdullah, H. Mokhlis, I. U. Haq, G. Fareed, and N. N. Mansor, "Fitness dependent optimizer-based automatic generation control of multi-source interconnected power system with non-linearities," *IEEE Access*, vol. 8, pp. 100989–101003, 2020.

[23] D. K. Lal and A. K. Barisal, "Grasshopper algorithm optimized fractional order fuzzy PID frequency controller for hybrid power systems," *Recent Adv. Electr. Electron. Eng. (Formerly Recent Patents Electr. Electron. Eng.)*, vol. 12, no. 6, pp. 519–531, Nov. 2019. [Online]. Available: http://www.eurekaselect.com/node/163836/article

[24] P. C. Pradhan, R. K. Sahu, and S. Panda, "Firefly algorithm optimized fuzzy PID controller for AGC of multi-area multi-source power systems with UPFC and SMES," *Eng. Sci. Technol., Int. J.*, vol. 19, no. 1, pp. 338–354, Mar. 2016.

[25] D. Yousri, T. S. Babu, and A. Fathy, "Recent methodology based Harris hawks optimizer for designing load frequency control incorporated in multi-interconnected renewable energy plants," *Sustain. Energy, Grids Netw.*, vol. 22, Jun. 2020, Art. no. 100352.

[26] M. Moazzami, G. B. Gharehpetian, H. Shahinzadeh, and S. H. Hosseinian, "Optimal locating and sizing of DG and D-STATCOM using modified shuffled frog leaping algorithm," in *Proc. 2nd Conf. Swarm Intell. Evol. Comput. (CSIEC)*, Mar. 2017, pp. 54–59.

[27] A. H. Yakout, W. Sabry, A. Y. Abdelaziz, H. M. Hasanien, K. M. AboRas, and H. Kotb, "Enhancement of frequency stability of power systems integrated with wind energy using marine predator algorithm based PIDA controlled STATCOM," *Alexandria Eng. J.*, vol. 61, no. 8, pp. 5851–5867, Aug. 2022. [Online]. Available: https://www.sciencedirect.com/science/article/

[28] Y. Arya, "Effect of electric vehicles on load frequency control in interconnected thermal and hydrothermal power systems utilising CF-FOIDF controller," *IET Gener., Transmiss. Distrib.*, vol. 14, no. 14, pp. 2666–2675, 2020. [Online]. Available: https://app.dimensions.ai/details/publication/pub.1125908032

[29] D. K. Lal, A. Barisal, and M. Tripathy, "Grey wolf optimizer algorithm based fuzzy PID controller for AGC of multi-area power system with TCPS," *Proc. Comput. Sci.*, vol. 92, pp. 99–105, Jan. 2016.

[30] N. Nayak, S. Mishra, D. Sharma, and B. K. Sahu, "Application of modified sine cosine algorithm to optimally design PID/fuzzy-PID controllers to deal with AGC issues in deregulated power system," *IET Gener., Transmiss. Distrib.*, vol. 13, no. 12, pp. 2474–2487, Jun. 2019.

[31] G. Chen, Z. Li, Z. Zhang, and S. Li, "An improved ACO algorithm optimized fuzzy PID controller for load frequency control in multi area interconnected power systems," *IEEE Access*, vol. 8, pp. 6429–6447, 2020.

[32] C. R. Reddy, B. S. Goud, F. Aymen, G. S. Rao, and E. C. Bortoni, "Power quality improvement in HRES grid connected system with FOPID based atom search optimization technique," *Energies*, vol. 14, no. 18, p. 5812, Sep. 2021. [Online]. Available: https://www.mdpi.com/1996-1073/14/18/5812

[33] A. Daraz, S. A. Malik, H. Mokhlis, I. U. Haq, F. Zafar, and N. N. Mansor, "Improved-fitness dependent optimizer based FOI-PD controller for automatic generation control of multi-source interconnected power system in deregulated environment," *IEEE Access*, vol. 8, pp. 197757–197775, 2020.

[34] V. Veerasamy, N. I. A. Wahab, R. Ramachandran, M. L. Othman, H. Hizam, A. X. R. Irudayaraj, J. M. Guerrero, and J. S. Kumar, "A Hankel matrix based reduced order model for stability analysis of hybrid power system using PSO-GSA optimized cascade PI-PD controller for automatic load frequency control," *IEEE Access*, vol. 8, pp. 71422–71446, 2020.

[35] A. Prakash, S. Murali, R. Shankar, and R. Bhushan, "HVDC tie-link modeling for restructured AGC using a novel fractional order cascade controller," *Electric Power Syst. Res.*, vol. 170, pp. 244–258, May 2019.

[36] D. Khamari, R. K. Sahu, T. S. Gorripotu, and S. Panda, "Automatic generation control of power system in deregulated environment using hybrid TLBO and pattern search technique," *Ain Shams Eng. J.*, vol. 11, no. 3, pp. 553–573, Sep. 2020.

[37] S. Kumari and G. Shankar, "Novel application of integral-tilt-derivative controller for performance evaluation of load frequency control of interconnected power system," *IET Gener., Transmiss. Distrib.*, vol. 12, no. 14, pp. 3550–3560, Aug. 2018.

[38] M. Ali, H. Kotb, K. M. Aboras, and N. H. Abbasy, "Design of cascaded PI-fractional order PID controller for improving the frequency response of hybrid microgrid system using gorilla troops optimizer," *IEEE Access*, vol. 9, pp. 150715–150732, 2021, doi: 10.1109/ACCESS.2021.3125317.

[39] H. M. Hasanien and A. A. El-Fergany, "Salp swarm algorithm-based optimal load frequency control of hybrid renewable power systems with communication delay and excitation cross-coupling effect," *Electr. Power Syst. Res.*, vol. 176, Nov. 2019, Art. no. 105938.

[40] S. Dhundhara and Y. P. Verma, "Capacitive energy storage with optimized controller for frequency regulation in realistic multisource deregulated power system," *Energy*, vol. 147, pp. 1108–1128, Mar. 2018.

[41] Y. Arya, "Impact of hydrogen Aqua electrolyzer-fuel cell units on automatic generation control of power systems with a new optimal fuzzy TIDF-II controller," *Renew. Energy*, vol. 139, pp. 468–482, Aug. 2019.

[42] J. M. Abdullah and T. Ahmed, "Fitness dependent optimizer: Inspired by the bee swarming reproductive process," *IEEE Access*, vol. 7, pp. 43473–43486, 2019.

[43] P. C. Chiu, A. Selamat, O. Krejcar, and K. K. Kuok, "Hybrid sine cosine and fitness dependent optimizer for global optimization," *IEEE Access*, vol. 9, pp. 128601–128622, 2021.

[44] D. Khamari, R. K. Sahu, T. S. Gorripotu, and S. Panda, "Automatic generation control of power system in deregulated environment using hybrid TLBO and pattern search technique," *Ain Shams Eng. J.*, vol. 11, no. 3, pp. 553–573, Sep. 2020.

AMIL DARAZ was born in Pakistan, in 1989. He received the B.E. degree in electronics engineering from COMSATS University Islamabad, Pakistan, in 2012, and the M.S. degree in power and control engineering and the Ph.D. degree in electrical engineering from the International Islamic University Islamabad (IIUI), Pakistan. His research interests include control systems, power system operation and control, and optimization of solving nonlinear problems.

SUHEEL ABDULLAH MALIK received the B.E. degree in electrical and electronics from Bangalore University, Bengaluru, India, in 1997, the M.S. degree in electronic engineering from Muhammad Ali Jinnah University (MAJU), Pakistan, and the Ph.D. degree in electronic engineering from the International Islamic University Islamabad (IIUI), Pakistan. Since 2007, he has been with IIUI, where he is currently working as the Chairperson/Associate Professor with the Department of Electrical Engineering (DEE). His research interests include control systems, numerical investigation of nonlinear problems, and application of nature-inspired metaheuristic algorithms for solving nonlinear problems.

AHMAD TAHER AZAR (Senior Member, IEEE) is a Research Professor at Prince Sultan University, Riyadh, Kingdom Saudi Arabia, and associate director of research and initiative center. He is a lab leader of Automated systems & Soft Computing Lab (ASSCL) at Prince Sultan University, Riyadh, Saudi Arabia. He is also a professor at the Faculty of Computers and Artificial intelligence, Benha University, Egypt. Prof. Azar is the Editor in Chief of the International Journal of System Dynamics Applications (IJSDA) and International Journal of Service Science, Management, Engineering, and Technology (IJSSMET), published by IGI Global, USA. He is also the Editor in Chief of the International Journal of Intelligent Engineering Informatics (IJIEI), Inderscience Publishers, Olney, UK. From 2018 to 2020, Prof. Azar was an associate editor of ISA Transactions, Elsevier. He is currently an associate editor for IEEE Systems Journal, Springer's Human-centric Computing and Information Sciences, and Elsevier's Engineering Applications of Artificial Intelligence. Prof. Azar has expertise in Control Theory and Applications, Robotics, Process Control, Artificial Intelligence, Machine Learning and dynamic system modeling. He has authored/co-authored over 350 research papers in prestigious peer-reviewed journals, book chapters, and conference proceedings.

SHERAZ ASLAM (Member, IEEE) received the B.S. degree in computer science from Bahauddin Zakariya University (BZU), Multan, Pakistan, in 2015, and the M.S. degree in computer science with a specialization in energy optimization in the smart grid from COMSATS University Islamabad (CUI), Islamabad, Pakistan, in 2018. He is currently pursuing the Ph.D. degree with the DICL Research Laboratory, Cyprus University of Technology (CUT), Limassol, Cyprus, under the supervision of Dr. Herodotos Herodotou, where he is also a part of EU-funded research project named as STEAM. He has worked as a Research Associate with Dr. Nadeem Javaid during his M.S. period at CUI. He has authored around 60 research publications in ISI-indexed international journals and conferences. His research interests include data analytics, generative adversarial networks, network security, wireless networks, smart grid, cloud computing, berth scheduling at maritime container terminal, se transportation, and intelligent shipping. He served/serving as a TPC member, a guest editor, an assistant editor, and an invited reviewer for international journals and conferences.

TAMIM ALKHALIFAH received the master's degree in CS from Swansea University, in 2009, and the Ph.D. degree in computer science from Flinders University, Adelaide, Australia, in 2018. He is currently working as an Assistant Professor with the Computer Department, College of Science and Arts in Ar Rass, Qassim University, Saudi Arabia. He has published several papers in the IT field. His primary research interests include e-technologies, mobile development, mobile learning, and gamification.

FAHAD ALTURISE received the Ph.D. degree in information technology from Flinders University. He is currently working as an Associate Professor with the Computer Department, College of Science and Arts in Ar Rass, Qassim University, Saudi Arabia. He has an experience of 12 years in the field of teaching and research. He has published 12 articles in international journals/conference proceedings. His primary research interests include e-learning, e-services, e-government, the IoT, ICT adaption, IT security, and software engineering. He was a member of the Australian Computer Society (ACS) for four years.

· · ·